Dynamic Fire Danger Mapping from Satellite Imagery and Meteorological Forecast Data

Paolo Fiorucci* and Francesco Gaetani

Centro Interuniversitario di Ricerca in Monitoraggio Ambientale, Università degli Studi di Genova e della Basilicata via Cadorna, Savona, Italy

Antonio Lanorte and Rosa Lasaponara

Istituto di Metodologie per l'Analisi Ambientale, Consiglio Nazionale delle Ricerche, Potenza, Italy

Received 8 March 2006; accepted 11 January 2007

ABSTRACT: This study aims at ascertaining if and how remote sensing data can improve fire danger estimation based on meteorological variables. With this goal in mind, a dynamic estimation of fire danger was performed using an approach based on the integration of satellite information within a comprehensive fire danger rating system. The performances obtained with and without using satellite data were carried out for fires that occurred during the fire season in the year 2003 in the Calabria region (southern Italy). This study area was selected, first, because it is highly representative of Mediterranean ecosystems and, second, because it is an interesting test case for wildfire occurrences within the Mediterranean basin.

The results obtained have shown that the use of satellite data reduced efficiently the overestimated danger areas, thus improving at least by 10% the fire

* Corresponding author address: Paolo Fiorucci, Centro Interuniversitario di Ricerca in Monitoraggio Ambientale, Università degli Studi di Genova e della Basilicata via Cadorna, 7, 17100 Savona, Italy.

E-mail address: paolo.fiorucci@unige.it

DOI: 10.1175/EI199.1

forecasting rate obtained without using satellite-based maps. Such findings can be directly extended to other similar Mediterranean ecosystems.

KEYWORDS: Fire danger estimation; Satellite; Meteorological forecast

1. Introduction

Every year, forest fires affect vast areas and cause devastating damage at European and global scales to such an extent that they are considered a very relevant factor of environmental degradation. Fire danger estimation plays an important role in the framework of programs for fire damage mitigation, as it provides quantitative information on the degree of degradation and/or stress experienced by plants, which can facilitate the ignition and spreading of fire (Lasaponara 2005) independently on the causes of ignition. The estimation of fire danger provides a valuable support for the designing of strategies related to the use and the distribution of the available fire fighting resources, which can prevent or at least minimize fire effects.

The most widely used fire danger forecasting systems are the Canadian Forest Fire Danger Rating System (CFFDRS; Stocks et al. 1989; Alexander et al. 1996; Van Nest and Alexander 1999; Lee et al. 2002) and the United States' National Fire Danger Rating System (NFDRS; Deeming et al. 1977; Anderson 1982). Over the years, both the CFFDRS and NFDRS have been used as baselines for the development of all analogous fire danger forecasting systems. All of these systems aim at the evaluation of the influence of topographical and meteorological variables on (i) the state of vegetation; (ii) potential wildfire behavior, that is, linear intensity (kW m^{-1}); and (iii) rate of spread (m h^{-1}).

Nevertheless, to provide reliable fire forecasting, all the existing fire danger systems should face a critical point represented by the characterization of the type of vegetation fuel. Such characterization should account for the structural components of vegetation and their response to fire behavior and fire propagation. First of all, dead and live fuels should be distinguished because they play a different role in the ignition and flammability. The physiological conditions of dead fuel lying on the forest floor (fallen branches, litter, and foliage) discriminate the capacity of a fire to spread over the territory because it is drier than live fuel and more dependent on rapid atmospheric changes. Live fuel has a marginal role in fire ignition, but it is critical in fire propagation because the amount of live moisture content is directly related to the rate of fire spread (Carlson and Burgan 2003; Sneeuwjagt and Peet 1985; Viegas 1998) In fact, in a fire propagation model both the load (kg m^{-2}) and lower heating value (LHV) (kJ kg^{-1}) of live fuels represent the major contribution to the fire-line intensity, that is, the energy emitted by the fire front during its propagation.

Moreover, it is widely recognized that (i) dead and (ii) live fuels are characterized by different dynamics of moisture content (Anderson 1982).

(i) Dead fuel moisture dynamics are significantly faster than those observed for live fuel. Dead fine vegetation exhibits moisture and density values dependent on rapid atmospheric changes and strictly linked to local meteorological conditions. For this reason, the estimation of dead fuel mois-

ture content is commonly based on meteorological variables and, therefore, the use of meteorological forecasts, obtained from reliable models, can provide useful information to simulate the effects of meteorological variables on dead vegetation moisture content and on the potential fire behavior.

(ii) Live fuel is much less dependent on atmospheric conditions as it can activate complex mechanisms to extract water from the soil reserve and reduce evapotranspiration. For these reasons, the application of meteorological variables for the estimation of live fuel moisture trends is very complex. That is the main reason why live fuel dynamics are generally considered quite constant for seasonal periods and in absence of significant disturbances, such as, pathologies or drought. Similar considerations can be made on the fuel load dynamics. Fuel load can be considered seasonally constant for forest stands; whereas, irregular changes from a live to dead state generally occur for some shrub species (i.e., Mediterranean maquis) and annual plants (herbaceous). Such changes modify the chemical and physical properties of plants and, therefore, their response to the ignition and the propagation of a fire front (Nunez-Regueria et al. 1999). Changes in physiological state are due both to external and phenological (induced by plant) phenomena, whose dynamics are difficult to represent through a mathematical modeling approach, especially in the case of a vast vegetated area. In this case, the use of information provided by satellite sensors can be efficiently used to recognize the actual state of fuels. For example, in some regions, such as the Mediterranean, where grasslands, pasturages, and shrub lands are the most common ignition points, the availability of satellite data can be crucial to perform a dynamic identification of irregular changes from a live to dead fuel state.

The widely used satellite-based index adopted for the estimation of the state of vegetation is the normalized difference vegetation index (NDVI). Such an index is obtained from the red and near-infrared (NIR) spectral bands as follows:

$$\mathrm{NDVI} = (\mathrm{NIR} - \mathrm{red})/(\mathrm{NIR} + \mathrm{red}). \quad (1)$$

The NDVI is indicative of plant photosynthetic activity (Fung 1997; Stoms and Hargrove 2000; Liang et al. 2005; Lasaponara and Masini 2006) and is related to the green leaf area index since it operates by contrasting intense chlorophyll pigment absorption in the red against the high reflectance of leaf mesophyll in the near infrared. Figure 1 shows the vegetation spectral signature, as well as the typical spectral behavior observed for healthy or stressed vegetation cover.

Variations in NDVI values suitably become indicative of variations in water and nutrient availability, plant disease, and other factors of stress, which in turn are indicators of a marked vulnerability of the vegetation to fire. For this reason, over the years, many authors have proposed the use of NDVI variations to assess the proneness of vegetation to fire (a detailed review is in Lasaponara 2005). Some results in the literature (Goward et al. 1990; Kogan 1990; Eidenshink et al. 1990; Burgan and Hartford 1993; Burgan et al. 1997) suggested that the absolute NDVI value might not provide a clear image of vegetation trends, since it is highly related

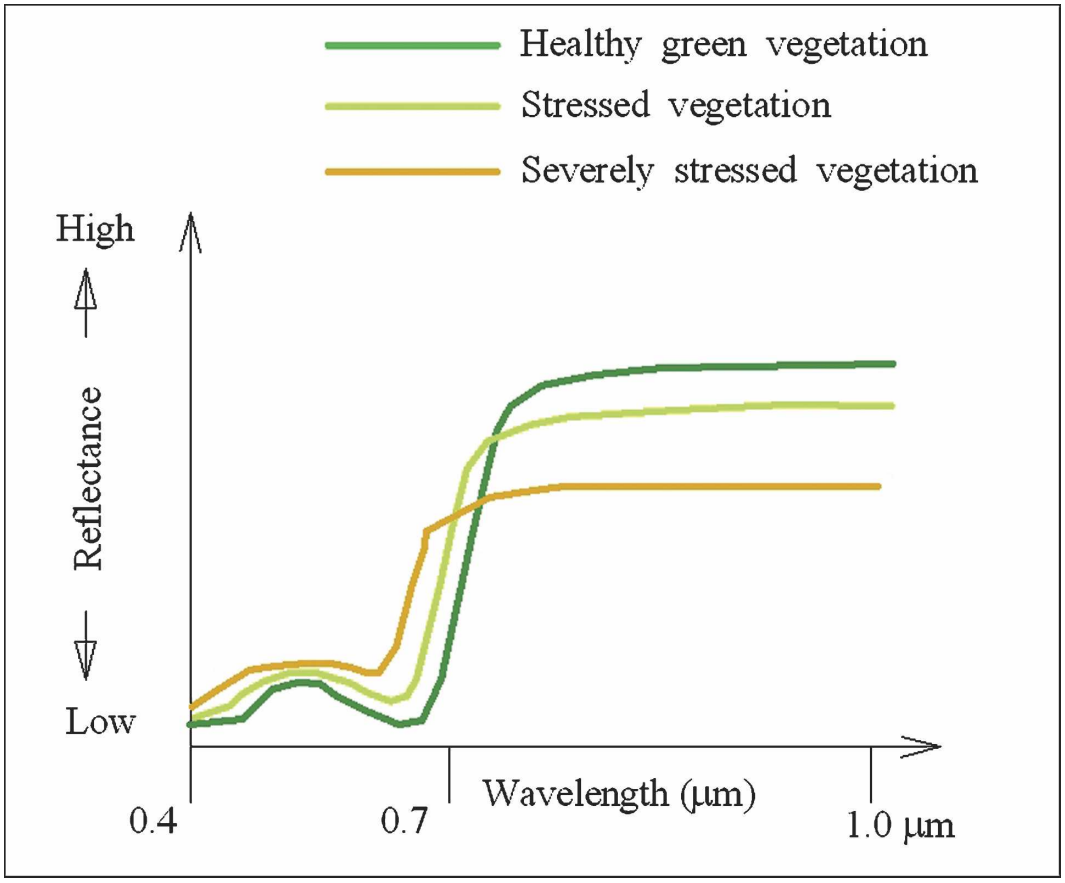

Figure 1. Vegetation spectral signature. The dark green line draws the spectral behavior observed for a given healthy and green vegetation cover; light green and orange lines draw the different spectral behavior observed, respectively, for stressed and severely stressed vegetation.

to landscape structure and to the amount of vegetation cover. Therefore, in order to isolate the weather-related component from the temporal variability of every pixel the same authors propose the use of greenness indexes (Eidenshink et al. 1990) that can be derived from NDVI as follows:

$$G^{\text{abs}} = (\text{ND}^0 - \text{ND}^{\text{min}})/\text{ND}^{\text{max}}, \tag{2}$$

where G^{abs} is the absolute percentage of greenness, ND^0 is the observed NDVI for a given pixel, and ND^{max} and ND^{min} are the maximum and the minimum NDVI values observed within a historical series of images for the same pixel.

The feasibility of the use of greenness indexes in order to estimate fire susceptibility has been tested by using both a comparison with fire occurrence (Barlette 2001) and fuel moisture content (Deshayes et al. 1998; Chuvieco et al. 2003) obtaining high satisfactory results for herbaceous plants.

To better discriminate the proportion of the load of dead fuel from live fuel,

Burgan et al. (Burgan et al. 1997) proposed the following equation, which introduces the relative greenness (RG) index:

$$\mathrm{RG} = (\mathrm{ND}^0 - \mathrm{ND}^{\min})/(\mathrm{ND}^{\max} - \mathrm{ND}^{\min}). \quad (3)$$

The effectiveness of RG for fire danger assessment was investigated by Barlette (Barletter 2001) in the United States where such an index showed high correlation values with fire occurrences. A quite popular fire danger index based on RG data is the fire potential index (FPI) developed by Burgan et al. in 1998 for the fire danger assessment of large areas. Such an index makes use of RG in order to calculate the percentage of live fuel load with respect to the total fuel load (namely, the live ratio). This information, along with data relevant to the moisture contents of fine dead fuel, gives a numeric index ranging from 1 to 100, which shows a good correlation with the potential danger of wildland fire. The methodology proposed in this paper follows similar lines to those briefly reported above, paying special attention to the integration of the satellite information within a comprehensive fire danger assessment system. In the rest of the paper, such a system will be introduced and described, highlighting the way the satellite data and the meteorological forecasts are used and integrated with reference to a specific case study.

2. Area of study and dataset

The Calabria region (southern Italy, 13°N, 36°E) represents an interesting area of study for wildfire occurrences within the Mediterranean basin (Figure 2). The complex topography of the region is based on microclimate conditions, which represent disturbance factors of the Mediterranean climate regime (i.e., hot dry summer and mild winter). The consequence of these geoclimatic variations is a heterogeneous mix of ecotypes and vegetation patches. The study area was selected by taking into consideration the high level of intensity, sensitivity, and presence of wild forest fires mainly during summer seasons. The high level of wildfire density characterizes the area as one of the most severely affected in Europe.

The considered study area was discretized into a uniform 250-m grid composed by $k = 1, \ldots, K$ cells. A digital elevation model (DEM) defined over the same grid was utilized to represent the aspect, slope, and elevation of the considered area. The vegetation cover was considered as composed by three main layers: a first layer ($i = 0$) representing the herbaceous plants and litter (fine fuels), a second layer ($i = 1$) populated by shrub and understorey, and a third top layer ($i = 2$) composed by the canopies of tall plants. In this study, only the *dead* fraction of vegetation in layer 0 is considered as fuel available for the ignition and the buildup of a fire, whereas layer 1 takes part only in the fire-line intensity evaluation. In fact, in this paper, only surface fires are modeled, and layer 2 is introduced as a mask layer. In this way, remote sensing data are used only where layer 0 is visible by satellite.

The vegetation cover description has been drawn from the Coordination of Information on the Environment (CORINE) Land Cover (CLC; European Commission 1994) map, which provides information on land cover on a 100-m grid

Figure 2. Area of study. (a) The Calabria region is highlighted in red on the Italian peninsula, whereas (b) the main classes provided by the CORINE Land Cover are represented using the DEM of the target region.

file. The CLC map uses a database comprising 44 categories, in accordance with standard European nomenclature, organized into five large classes: artificial surfaces, agricultural areas, forest and seminatural areas, wetlands, and water bodies. For each CLC category, four seasonal parameter values were obtained, on the basis of relevant literature (Anderson 1982; Nunez-Regueira et al. 1999). Such parameters are the nominal loads or densities (kg m^{-2}) of the three layers, the LHV

Figure 2. (*Continued*)

(kJ kg^{-1}) of perennial fuels (layers 1 and 2), and the higher heating value (HHV) (kJ kg^{-1}) of annual fuel (layer 0). The moisture contents of perennial fuels are assumed constant over seasonal periods. The evaluation of fuel loads requires consistent and detailed information that, at least at a wide spatial scale, is often unfeasible. However, the effectiveness of remote sensing and meteorological models for water stress assessment and wild land fire risk assessment has been recognized (Burgan et al. 1998; Sebastian Lopez et al. 2002; Caetano et al. 2004). Thus, only the moisture dynamics of dead fine annual fuel is modeled, whereas the dead fine and shrub fuel load is estimated through satellite data.

The satellite RG maps used for this study were obtained from a temporal series of NDVI SPOT-VEGETATION spanning from 1998 to 2003. Such NDVI data are publicly available at the Web site of Vlaamse Instelling voor Technologisch Onderzock (VITO) Image Processing center (Mol, Belgium; http://www.vgt.vito.be). The investigations were performed using the satellite time series data made up

of maximum value composite (MVC) of NDVI performed over a 10-day period (decadal): S10. Historical maximum and minimum NDVI maps for the study area were produced on a pixel basis by extracting the highest and lowest values observed from the MVC–NDVI maps recorded over the considered 6-yr period. These NDVI values were then composed into maximum and minimum maps and used with current 10-day composition NDVI maps to perform the relative greenness calculations. Note that pixels affected by snow, clouds, and residual atmospheric contamination were detected and excluded.

The meteorological data used by the system are those relevant to the daily forecasts produced by the meteorological nonhydrostatic Limited-Area Model (LAM) Lokal Modell (Doms and Schättler 1999) and provided by the Regional Environmental Protection Agency of Bologna to Civil Protection. The LAM provides a set of 0.05° grid data discretized in time steps of 3 h over a time horizon of 72 h. The considered information is the 3-h cumulated rainfall, the air temperature, the dewpoint temperature, and the wind speed and direction.

3. Methods

The proposed procedure has been implemented upon a specific existing dynamic wildfire danger assessment system. Such a system (Fiorucci et al. 2004; Fiorucci et al. 2006), fully operative since 2003 at the Italian Civil Protection headquarters, follows reasoning lines similar to those introduced by the developers of the Canadian and U.S. systems. A schematic representation of the system architecture is given in Figure 3. The system can be considered as composed by two main modules. The first (Fig. 3a) provides the dynamics relevant to the fine fuel moisture conditions, whereas a potential fire spread model (Fig. 3b) is used to evaluate the potential behavior of the wildfire front in terms of rate of spread and fire-line intensity.

If layer 2 is present on cell k, the dead fine fuel loads of the lower layers are defined by their seasonal values $\hat{\delta}_k^{0,1}$. In absence of layer 2, the fuel load of layer 0 is a parameter, whose value at time instant t in cell k, $\delta_k^0(t)$ is derived from a seasonal value $\hat{\delta}_k^0$ through the $\mathrm{RG}_k(t)$ observed in cell k and relevant to time instant t.

$$\delta_k^0(t) = [1 - \mathrm{RG}_k(t)]\hat{\delta}_k^0, \tag{4}$$

where $k = 1, \ldots, N$ and $t = 1, \ldots, T$.

Fuel moisture content (FMC) dynamics of dead fine fuel was modeled on the basis of the assumption that the moisture content of a particle of dead fuel, within a system with constant temperature and humidity, increases or decreases until, eventually, a value denoted as equilibrium moisture content (EMC) is reached. EMC is a function of the air temperature and relative humidity close to the fuel (Catchpole et al. 2001). The basic model used to represent such a dynamic behavior is (Byram 1973)

$$\frac{d\mathrm{FMC}(t)}{dt} = K_1 - K_2\,\mathrm{FMC}(t), \tag{5}$$

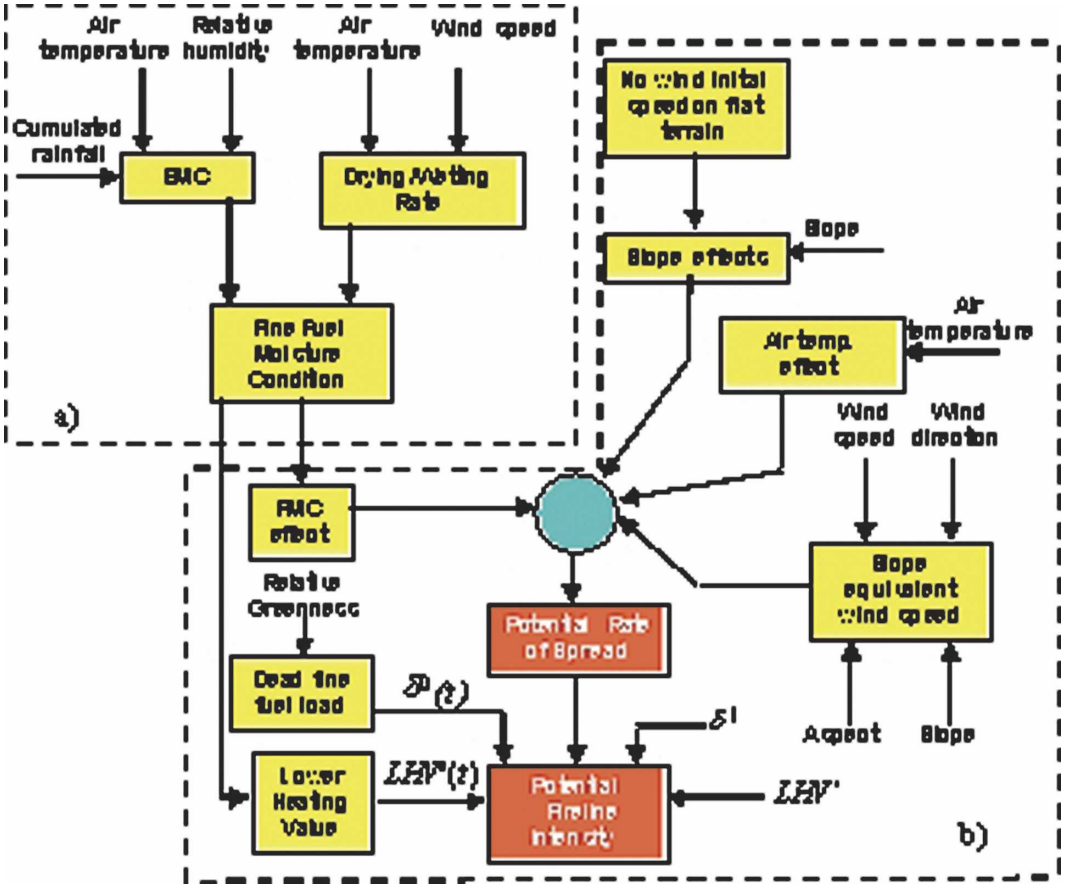

Figure 3. (a) Dynamics relevant to the fine fuel moisture conditions. (b) Potential fire spread model.

where FMC(t) corresponds to the fuel moisture contents at time t, whereas K_1 and K_2 are suitable constants to be estimated. Note that in this model K_1/K_2 represents the asymptotic value (i.e., EMC), whereas $1/K_2$ is the drying/wetting rate that is the time constant of the first-order system (5). Several techniques can be found in the literature to evaluate EMC (Catchpole et al. 2001). Such models were derived and calibrated on the basis of extensive data collection and tests carried out on local forest vegetation for several years. The model implemented within the considered system to express the dependence of the EMC on meteorological variables (air temperature, relative humidity, and cumulated rainfall) has a simpler structure (and a lower number of parameters) than most of the well-known ones used in the literature (Fiorucci et al. 2004).

The potential rate of spread $v_k(t)$ at time instant t in cell k is given by a model that takes into account the influence of meteorological variables (air temperature and wind speed and direction) and topography (slope and aspect) on an initial given value of rate of spread on flat terrain in the absence of wind (see Fiorucci et al. 2004).

The distribution of $v_k(t)$ in space and time gives a measure of the capacity of a

fire to grow after an ignition. However, the potential fire-line intensity (kW m^{-1}), whose value is linearly dependent on the potential rate of spread of a wildfire, is the most significant variable for fire danger classification, since its value is strictly related to the efforts necessary to extinguish a fire (Rothermel 1983).

In this study, the original Byram's equation (Byram 1973) was conveniently modified to determine the fire-line intensity $I_k(t)$ (kW m^{-1}) taking into account the actual availability of dead fuel on cell k, namely,

$$\begin{cases} I_k(t) = \upsilon_k(t)[\delta_k^0(t)\mathrm{LHV}_k^0(t) + \hat{\delta}_k^1\mathrm{LHV}_k^1(t)] & \text{if cell } k \text{ is not covered by layer 2} \\ I_k(t) = \upsilon_k(t)[\hat{\delta}_k^0\mathrm{LHV}_k^0(t) + \hat{\delta}_k^1\mathrm{LHV}_k^1] & \text{otherwise,} \end{cases} \tag{6}$$

where $k = 1, \ldots, N$, $t = 1, \ldots, T$ and LHV_k^0 and LHV_k^1 are the lower heating values (kJ kg^{-1}) of layers 0 and 1 in cell k, given by

$$\mathrm{LHV}_k^0(t) = \mathrm{HHV}_k^0\left[1 - \frac{\mathrm{FMC}_k(t)}{100}\right] - Q\frac{\mathrm{FMC}_k(t)}{100}, \tag{7}$$

where $k = 1, \ldots, N$, $t = 1, \ldots, T$ and

$$\mathrm{LHV}_k^1 = \mathrm{HHV}_k^1\left(1 - \frac{\tilde{u}_k}{100}\right) - Q\frac{\tilde{u}_k}{100}, \tag{8}$$

where $k = 1, \ldots, N$, $t = 1, \ldots, T$. HHV_k^0 and HHV_k^1 (kJ kg^{-1}) are relevant to fine dead fuel and live fuel, respectively, and have been evaluated on the basis of the botanical structure (prevailing species, degree of vegetation curing, and density) in cell k, Q is the latent heating value (kJ kg^{-1}), and $\tilde{u}_k$ is the moisture contents of live fuel in cell k.

The term RG, whose values are less or equal to 1, introduces a reduction factor $\hat{\delta}_k^0$, which implies a reduction of the forecasted fire-line intensity and, therefore, a decreasing number of cells belonging to high-level risk classes.

4. Results

The validation procedure was carried out considering a specific dataset relevant to the actual fires that occurred in the Calabria region during the summer season in the year 2003. This set refers to 1102 wild land fires detected from 21 March to 21 September 2003 (Corpo Forestale dello Stato 2003). The dataset was classified according to four different classes of burnt area, namely, E_s ($s = 1, \ldots, 4$), as defined on the basis of the area S affected by each fire. Table 1 shows, for each class E_s, the number of fires that occurred, burnt areas, and fire duration. Burnt areas and fire duration are reported in Table 1 using both an integral measure and an average value per fire. Wildfires are also classified according to the season (spring/summer) in which they occurred. Such distinction highlights the influence that the state of fuel has on the occurrence of fire. Table 1 shows that the number of wildfires is almost negligible in spring (21 March–21 June). In fact, in such a period, the percentage of dead fuel load for each cell reaches its minimum.

The information obtained from Table 1 was used to validate the outputs generated by the wild land danger assessment system in two different configurations:

Table 1. Classification of the considered wildfire dataset. Each event that occurred within the study area (measured in km^2) has been classified on the basis of its burnt area. In the table the number of wildfires of each class, along with some statistical data, are reported.

Class (km^2)			E_1 ($S \leq 0.01$)	E_2 ($0.01 < S \leq 0.1$)	E_3 ($0.1 < S \leq 1$)	E_4 ($S > 1$)	All classes
Number of occurred fires	Spring		14	49	3	0	66
	Summer		174	697	163	8	1042
Burnt area S (km^2)	Spring	Integral value	0.064	1.707	0.640	0	2.410
		Average per fire	0.005	0.034	0.213	0	0.037
	Summer	Integral value	0.652	22.766	36.196	12.720	72.340
		Average per fire	0.004	0.033	0.222	1.590	0.690
Fire duration (h)	Spring	Integral value	71.55	363	23.75	0	458.30
		Average per fire	5.11	7.26	7.91	0	6.87
	Summer	Integral value	560.47	43.984	2706.17	179.20	7844.26
		Average per fire	3.22	0.063	16.64	22.40	7.53

1) by using RG to reduce the dead fine fuel load, and 2) by assuming a seasonal constant value of dead fine fuel load. The validation procedure is based on the discretization of the forecasted fire-line intensity $I_k(t)$ within five danger classes, R_j ($j = 0, \ldots, 4$) (see Table 2). In such a manner, each wildfire is characterized by two (comparable) parameters, that is, class E_s given by its burnt area, and class R_j given by the value of fire-line intensity of the cell k where such a fire occurred.

A first evaluation of the system was carried out on its ability to identify the correct danger class with reference to the burnt area of the actual fires. In Figure 4 a representation of the results obtained by the system through satellite data during summer is reported. From Figure 4 one can observe that the number of errors of the system, that is, wildfires that occurred in the cells classified in the classes $j = 0$ and $j = 1$, is very low (69 wildfires) and their average burnt area and time duration are limited too. The accomplishment of this fundamental point allows us to concentrate on a more ambitious objective: the ability of the system to classify the considered area in terms of the real fire danger. This is achieved through a sharp reduction of the number of the cells classified within the medium danger class, containing the largest number of cells. Through the satellite data some cells of the medium danger class are classified in the two lower ones.

The index n_{sj}, for $s = 1, \ldots, 4$, $j = 0, \ldots, 4$ was introduced in order to evaluate the number of fires belonging to class s and characterized by danger j. For each fire belonging to class s, the index n_{sj} was computed, taking into account the danger index j equal to the value of the highest danger class (achieved by the cell where the fire has occurred).

Table 2. The danger relevant to a generic cell *k* was introduced on the basis of its fire-line intensity value. Five danger classes were introduced in accordance with the thresholds defined by Rothermel (Rothermel 1983) in relation to the effort that would be required to suppress the fires.

Danger classes	R_0	R_1	R_2	R_3	R_4
Lower bound (kW m^{-1})	0	86	345	900	1800
Upper bound (kW m^{-1})	86	345	900	1800	>1800

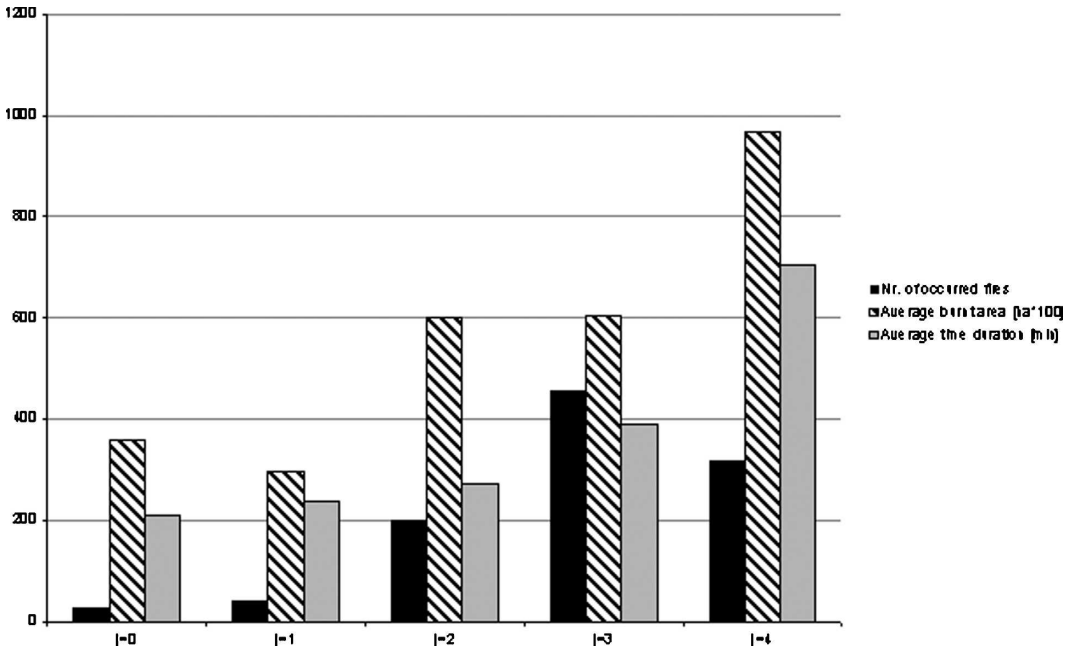

Figure 4. An analysis of the system performances improved with RG data during the summer season. In the chart, the number of fires that occurred, the average burnt area per fire, and the average time duration per fire are reported for each danger classes $j = 0, \ldots, 4$.

It was then possible to introduce the following performance index:

$$\Psi = \sum_{s=1}^{4} \sum_{j=0}^{4} \xi_{sj} n_{sj}. \tag{9}$$

Parameters ξ_{sj}, where $0 \leq \xi_{sj} \leq 1$, evaluate the occurrence of a fire classified in class E_s within a cell denoted by danger class R_j. The value of such parameters is minimum (i.e., 0) if the extension class s of the considered fire is the same as the danger class j in which the fire occurred. Fires classified in class $s \neq j$ are penalized by parameters $\xi_{sj} > 0$. The worst performance achievable by the system is the one expressed by the parameter $\xi_{sj} = 1$. Also, in case of fires that occurred within cells denoted by danger class $j = 0$ (null danger), parameters ξ_{sj} are set to 1 independently from the extension class s. On this basis, the values reported in Table 3 have been selected according to the coefficients appearing in (9).

Table 3. Parameters ξ_{sj} are introduced in the validation procedure aiming at weighing the occurrence of wildfires of area s within cells denoted by danger j.

ξ_{sj}	$j = 0$	$j = 1$	$j = 2$	$j = 3$	$j = 4$
$s = 1$	1.0	0.0	0.2	0.4	0.8
$s = 2$	1.0	0.8	0.0	0.4	0.6
$s = 3$	1.0	1.0	0.4	0.0	0.2
$s = 4$	1.0	1.0	0.6	0.2	0.0

Table 4. The values of the performance index Ψ for the two considered seasons in the two different configurations of the system.

Ψ			
	Spring	RG	14.0
		No RG	14.4
	Summer	RG	393.2
		No RG	393.8

With reference to the data reported in Table 1, if the system had classified all the cells in the danger class 0, the worst possible value of Ψ would have been $\Psi = 66$ in spring and $\Psi = 1042$ in summer. Such latter values represent the overall number of fires that occurred in the considered period of time. In Table 4, the performance index Ψ for spring and summer wildfires relevant to extension classes E_s ($s = 1, \ldots, 4$), and danger classes R_j ($j = 0, \ldots, 4$) for the two configurations of the system is reported.

In Table 4 it is evident that the first objective of the system, which is its ability to identify the correct danger classes according to the area of the fires, is not penalized by the introduction of RG data in the system. In fact, in this study, RG data have been introduced only to reduce the number of cells where the fuel state is compatible with a successful ignition (i.e., where the fuel is not vascularized). The effectiveness of the system with RG data increases significantly in connection to the capacity of defining areas characterized by the highest danger classes. In fact, an analysis of the distribution of the percentage of cells among the different danger classes j (see Table 5) shows a considerable increase of cells belonging to classes $j = 0, 1$ and, consequently, a significant shift of cells from high-danger classes to lower-danger classes. Such behavior is noticeable in summer, when the amount of dead fuel increases.

In Table 5, it is worth observing that in springtime, when the RG reaches its maximum annual value, the number of cells falling in classes 2, 3, and 4 (medium and high danger) decreases about 13% if remote sensing observations are introduced in the system. Besides, in summer, when the annual fuel is partially cured and RG in layer 0 reaches its minimum annual value, the percentage of cells that shift from high- (2, 3, 4) to lower- (0, 1) danger classes is about 10%.

Overall results from the evaluation process showed that the introduction of RG in the fire danger forecasting model provides a minimum improvement of 10% of the forecasting rate compared to results obtained without using satellite RG maps, thus maintaining exactly the same satisfactory performance in terms of the number of predicted fires.

A significant performance index that can be considered to evaluate the inclusion

Table 5. Classification of the considered area of study. For the two fire seasons considered and for the two configurations of the system (with RG and without RG) the percentages of cells classified for each danger indexes *j* are reported.

		$j = 0$	$j = 1$	$j = 2$	$j = 3$	$j = 4$
Spring	RG	24.69	19.08	19.41	23.32	13.48
	No RG	19.63	11.70	28.58	25.93	14.14
Summer	RG	17.18	13.28	19.68	25.32	24.52
	No RG	13.08	8.66	24.88	27.89	25.49

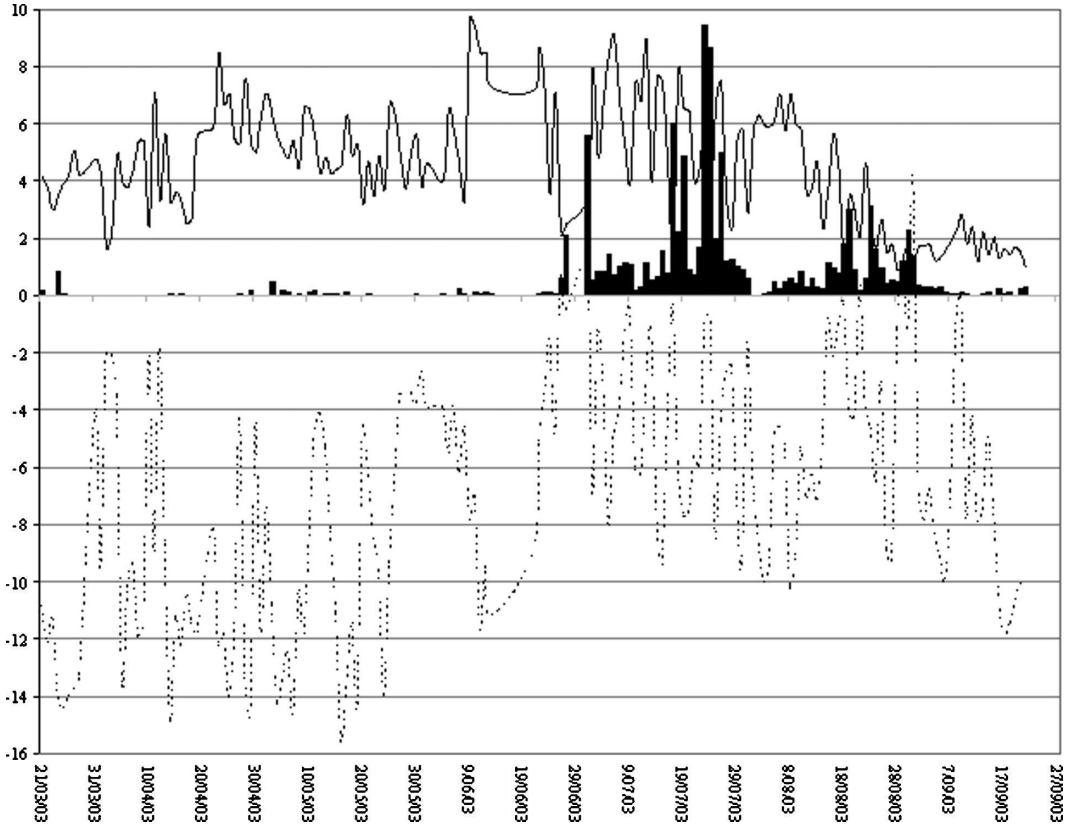

Figure 5. A representation of the performances attainable by the system in the two different configurations. The dotted line represents the difference between the percentages of cells classified in class $j = 2$ in the two different configurations. The dashed line represents the difference between the percentages of cells classified in class $j = 0$ (lowest-danger class) in the two different configurations. The bars represent the daily percentage of total burnt area (see Table 5).

of RG in the system is given by the difference between the percentage of cells belonging to a given class j in the two different configurations.

In Figure 5, such differences in the case of classes 0 and 2 and the daily percentage of the total burnt area are reported for all of the considered period. Figure 5 clearly shows the effect that RG has on the quality of the prediction. In fact, in the case of low wildfire activity, the percentage of cells shifting from class 2 to lower classes (e.g., class 0) is remarkable. Also in the periods of maximum wildfire activity (i.e., summer) the use of RG in the system still allows the reclassification of some cells.

5. Conclusions

In the paper, an integrated approach for fire danger assessment of wide geographical areas based on SPOT-VEGETATION satellite data and meteorological

forecast data is presented and discussed. The paper describes the architecture of the overall system and, in particular, the various models on which the hazard assessment is based. Satellite data are introduced in the system aiming at characterizing the phenology of the considered fuel. In this circumstance, RG values are used in order to identify the actual fine fuels state and, therefore, the proper dynamics to be used to model their physiological characteristics (FMC). Such information allows characterization of the actual fire-line intensity, which represents the danger level within an incoming time interval of suitable length.

The benefits achievable by the introduction of the proposed approach in the fire-fighting operational chain are apparent. In fact, success in the suppression phase is strictly related to the promptness of the first intervention (initial attack). In fact, since the number of (ground-based) resources is generally scarce and their dynamics is slow, one can think to relocate the resources near the zones that present a very high and persistent forecasted danger.

In this case, because of the high operational costs of relocation, the application of the proposed method, along with reliable meteorological forecasts or observations, allows decision makers to exclude a priori a considerable percentage of the territory (in the considered case study about 30% in summer) from the areas that must be subjected to preoperational actions (patrolling, resources relocation, and introducing rules and regulations for agricultural practices).

Results from the evaluation process showed that the dynamic evaluations performed by using RG allows us to reduce at least by 10% the areas classified as fire vulnerable, thus maintaining the same satisfactory performance in terms of the number of predicted fires.

Acknowledgments. This research was funded by Italian National Civil Protection in the context of "PROSCENIO-Fire Project" and supported by the European Space Agency (ESA) in the context of "Fire susceptibility estimation in the Mediterranean ecosystems by using AATSR, MODIS, VEGETATION and AVHRR data," No. 1503, category 1 project. The authors thank the Italian National Forest Service for providing forest fire data that have made this study possible.

References

Alexander, M. E., B. J. Stocks, and B. D. Lawson, 1996: The Canadian Forest Fire Danger Rating System. *Initial Attack,* Spring Issue, 5–8.

Anderson, H. E., 1982: Aids to determining fuel models for estimating fire behavior. USDA, Forest Service, General Tech. Rep. INT-122, Intermountain Forest and Range Experiment Station, Ogden, UT, 22 pp.

Barlette, R. A., 2001: Using the Normalized Difference of Vegetation Index from AVHRR imagery for fire potential assessment in the United States. *Proc. 3d Int. Workshop on Remote Sensing and GIS Applications to Forest Fire Management—New Methods and Sensors,* Paris, France, Alcala´: EARSeL, 19–21.

Burgan, R. E., and R. A. Hartford, 1993: Monitoring vegetation greenness with satellite data. USDA, Forest Service, General Tech. Rep. INT-297, Intermountain Research Station, Ogden, UT, 43 pp.

——, P. L. Andrews, L. S. Bradshaw, C. H. Chase, R. A. Hartford, and D. J. Latham, 1997: Current status of the wildland fire assessment system (WFAS). *Fire Manage. Notes,* **57,** 14–17.

——, R. W. Klaver, and J. M. Klaver, 1998: Fuel models and fire potential from satellite and surface observations. *Int. J. Wildland Fire,* **8,** 159–170.

Byram, G. M., 1973: Combustion of forest fuels. *Forest Fire: Control and Use,* K. P. Davis, Ed., McGraw-Hill, 61–89.

Caetano, M. R., S. Freire, and H. Carrão, 2004: Fire risk mapping by integration of dynamic and structural variables. *Remote Sensing in Transition,* R. Goossens, Ed., Millpress, 319–326.

Carlson, J. D., and R. E. Burgan, 2003: Review of user needs in operational fire danger estimation: The Oklahoma example. *Int. J. Remote Sens.,* **24,** 1601–1620.

Catchpole, E. A., W. R. Catchpole, N. R. Viney, W. L. McCaw, and J. B. Marsden-Smedley, 2001: Estimating fuel response time and predicting fuel moisture content from field data. *Int. J. Wildland Fire,* **10,** 215–219.

Chuvieco, E., I. Aguado, D. Cocero, D. And, and O. Rian, 2003: Design of an empirical index to estimate fuel moisture content from NOAA-AVHRR images in forest fire danger studies. *Int. J. Remote Sens.,* **24,** 1621–1637.

Corpo Forestale dello Stato, 2003: Foglio Notizie Antincendio Boschivo. Tech. Rep., Rome, Italy, 109 pp.

Deeming, J. E., R. E. Burgan, and J. D. Cohen, 1977: The National Fire-Danger Rating System—1978. USDA, Forest Service, General Tech. Rep. INT-39, Intermountain Forest and Range Experiment Station, Ogden, UT, 63 pp.

Deshayes, M., E. Chuvieco, E. Cocero, M. Karteris, N. Koutsias, and N. Stach, 1998: Evaluation of different NOAA-AVHRR derived indexes for fuel moisture content estimation: Interest for short term fire risk assessment. *Proc. 3d Int. Conf. on Forest Fire Research,* Coimbra, Portugal, ADAI, 1149–1167.

Doms, G., and U. Schättler, 1999: The Non-Hydrostatic Limited-Area Model LM (Lokal-Modell) of DWD. Tech. Rep., Deutscher Wetterdienst, Offenbach, Germany, 174 pp. [Available online at http://www.cosmo-model.org/public/documentationVer1.htm#sc_doc.]

Eidenshink, J. C., R. E. Burgan, and R. H. Haas, 1990: Monitoring fire fuels condition by using time series composites of Advanced Very High Resolution Radiometer (AVHRR) data. *Proc. Resource Technology 90,* Washington, DC, ASPRS, 68–82.

European Commission, 1994: CORINE land cover—Technical guide. Publication EUR 12585, EG, DG Environment, Nuclear Safety, and Civil Protection, Luxembourg, Luxembourg. [Available online at http://reports.eea.europa.eu/COR0-landcover/en/land_cover.pdf.]

Fiorucci, P., F. Gaetani, and R. Minciardi, 2004: An integrated system for the forest fires dynamic hazard assessment over a wide area. *Proc. iEMSs 2004 Int. Congress: Complexity and Integrated Resources Management,* Osnabrueck, Germany, International Environmental Modelling and Software Society, CD-ROM.

——, ——, ——, and A. Scipioni, 2006: RISICO: A system for dynamic wildfire risk assessment in Italy. *Proc. Fifth Int. Conf. on Forest Fire Research,* D. X. Viegas, Ed., Figuera da Foz, Portugal, CD-ROM.

Fung, I., 1997: Climate change: A greener north. *Nature,* **386,** 659–660.

Goward, S. N., B. Markham, D. G. Dye, W. Dulaney, and J. Yang, 1990: Normalized difference vegetation index measurements from the advanced very high resolution radiometer. *Remote Sens. Environ.,* **35,** 257–277.

Kogan, F. N., 1990: Remote sensing of weather impacts on vegetation in nonhomogeneous areas. *Int. J. Remote Sens.,* **11,** 1405–1419.

Lasaponara, R., 2005: Inter-comparison of AHVRR-based fire susceptibility indicators for the Mediterranean ecosystems of Southern Italy. *Int. J. Remote Sens.,* **26,** 853–870.

——, and N. Masini, 2006: Identification of archaeological buried remains based on Normalized Difference Vegetation Index (NDVI) from Quickbird satellite data. *IEEE Geosci. Remote Sens. Lett.,* **3,** 325–328.

Lee, B. S., M. E. Alexander, B. C. Hawkes, T. J. Lynham, B. J. Stocks, and P. Englefield, 2002: Information systems in support of wildland fire management decision making in Canada. *Comput. Electron. Agric.,* **37,** 185–198.

Liang, E. Y., X. M. Shao, and J. C. He, 2005: Relationship between tree growth and NDVI of grassland in the semiarid grassland of north China. *Int. J. Remote Sens.,* **26,** 2901–2908.

Nunez-Regueira, L., J. Rodriguez, J. Proupin, and B. Mourino, 1999: Design of forest biomass energetic maps as a tool to fight forest wildfires. *Termochimica Acta,* **328,** 111–120.

Rothermel, R. C., 1983: How to predict the spread and intensity of forest and range fires. USDA, Forest Service, General Tech. Rep. INT-143, Intermountain Forest and Range Experiment Station, Ogden, UT, 161 pp.

Sebastian Lopez, A., J. San-Miguel-Ayanz, and R. Burgan, 2002: Integration of satellite sensor data, fuel type maps and meteorological observations for evaluation of forest fire risk at the pan-European scale. *Int. J. Remote Sens.,* **23,** 2713–2719.

Sneeuwjagt, R. J., and G. B. Peet, 1985: Forest fire behavior tables for Western Australia. 3d ed. Western Australia Department of Conservation and Land Management, Perth, Australia, 50 pp.

Stocks, B. J., B. D. Lawson, M. E. Alexander, C. E. van Wagner, R. S. McAlpine, T. J. Lynham, and D. E. Dube, 1989: The Canadian forest fire danger rating system: An overview. *For. Chron.,* **65,** 450–457.

Stoms, D. M., and W. W. Hargrove, 2000: Potential NDVI as a baseline for monitoring ecosystem functioning. *Int. J. Remote Sens.,* **21,** 401–407.

Van Nest, T. A., and M. E. Alexander, 1999: Systems for rating fire danger and predicting fire behavior used in Canada. *Proc. Natl. Interagency Fire Behavior Workshop,* Phoenix, AZ, 13 pp.

Viegas, D. X., 1998: Fuel moisture evaluation for fire behaviour assessment. *Proc. Advanced Study Course on Wildfire Management: Final Report,* G. Eftichidis, P. Balabaris, and A. Ghazi, Eds., Marathon, Greece, European Union, 81–92.